Environmental Science & Technology

Article

Cite This: Environ. Sci. Technol. 2019, 53, 6192−6202

pubs.acs.org/est

Molecular Characterization and Source Identification of Atmospheric Particulate Organosulfates Using Ultrahigh Resolution Mass Spectrometry

Kai Wang,[†,‡,#] Yun Zhang,[‡] Ru-Jin Huang,[*,†,§] Meng Wang,[†] Haiyan Ni,[†] Christopher J. Kampf,[∥,⊥] Yafang Cheng,[∥] Merete Bilde,[#] Marianne Glasius,[#] and Thorsten Hoffmann[‡]

[†]Key Laboratory of Aerosol Chemistry and Physics, State Key Laboratory of Loess and Quaternary Geology, and Center for Excellence in Quaternary Science and Global Change, Institute of Earth Environment, Chinese Academy of Sciences, Xi'an 710061, China

[‡]Institute of Inorganic and Analytical Chemistry, Johannes Gutenberg University Mainz, Duesbergweg 10−14, 55128 Mainz, Germany

[§]Open Studio for Oceanic-Continental Climate and Environment Changes, Pilot National Laboratory for Marine Science and Technology (Qingdao), Qingdao 266061, China

[∥]Multiphase Chemistry Department, Max Planck Institute for Chemistry, Hahn-Meitner-Weg 1, 55128 Mainz, Germany

[⊥]Institute of Organic Chemistry, Johannes Gutenberg University Mainz, Duesbergweg 10−14, 55128 Mainz, Germany

[#]Department of Chemistry, Aarhus University, Langelandsgade 140, DK-8000 Aarhus C, Denmark

Supporting Information

ABSTRACT: Organosulfates (OSs) have been observed as substantial constituents of atmospheric organic aerosol (OA) in a wide range of environments; however, the chemical composition, sources, and formation mechanism of OSs are still not well understood. In this study, we first created an "OS precursor map" based on the elemental composition of previous OS chamber experiments. Then, according to this "OS precursor map", we estimated the possible sources and molecular structures of OSs in atmospheric $PM_{2.5}$ (particles with aerodynamic diameter ≤ 2.5 μm) samples, which were collected in urban areas of Beijing (China) and Mainz (Germany) and analyzed by ultrahigh-performance liquid chromatography (UHPLC) coupled with an Orbitrap mass spectrometer. On the basis of the "OS precursor map", together with the polarity information provided by UHPLC, OSs in Mainz samples are suggested to be mainly derived from isoprene/glyoxal or other unknown small polar organic compounds, while OSs in Beijing samples were generated from both isoprene/glyoxal and anthropogenic sources (e.g., long-chain alkanes and aromatics). The nitrooxy-OSs in the clean aerosol samples were mainly derived from monoterpenes, while much fewer monoterpene-derived nitrooxy-OSs were obtained in the polluted aerosol samples, showing that nitrooxy-OS formation is affected by different precursors in clean and polluted air conditions.

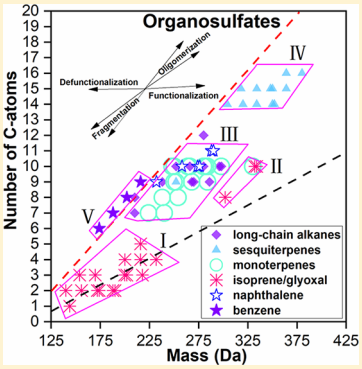

INTRODUCTION

Organic aerosol (OA) accounts for an important fraction (20−90%) of submicron atmospheric particulate mass[1,2] and influences global climate, air quality, and human health.[3−6] Atmospheric OA can be divided into two categories. Primary OA (POA) is directly emitted into the atmosphere from biogenic or anthropogenic sources; whereas secondary OA (SOA) is formed in the atmosphere through gas-to-particle conversion.[7] Due to a wide variety of natural and anthropogenic sources as well as the complex multiphase chemical reactions, organic compounds in OA present a large space of physicochemical properties, including hydrocarbons, alcohols, carboxylic acids, organosulfates (OSs), and organonitrates. Hence, characterizing the chemical composition of the organics in OA is a challenging but vital task.[8−12]

Recently, OSs have been observed as an important fraction in the ambient OA.[10,11,13−21] Due to the presence of a deprotonated functional group R−O−SO_3^-, OSs are acidic and highly water-soluble and therefore may affect the surface activity and hygroscopic properties of the atmospheric particles, leading to potential impacts on climate.[22] To understand the sources, formation process, and chemical composition of OSs, several laboratory smog chamber studies have been conducted. In the presence of acidified sulfate aerosol seed, OSs have been produced in the chamber studies from O_3, OH, or NO_3 oxidation of biogenic volatile organic compounds (VOCs), such as isoprene, monoterpenes,

Received: May 1, 2019
Accepted: May 13, 2019
Published: May 14, 2019

DOI: 10.1021/acs.est.9b02628
Environ. Sci. Technol. 2019, 53, 6192−6202

sesquiterpenes, and unsaturated aldehydes.[23−26] Recently, OSs derived from aromatics and long-chain alkanes have been studied to understand the effect of anthropogenic sources on OS formation.[27,28] However, due to a lack of authentic standards, identification and quantification of OSs is still a challenging task,[19] which further results in the difficulty to understand the sources and formation pathways of OSs.

Previous studies on OSs were conducted mainly in Europe and USA[13,14,17,23,24,29−33] and only a few in China.[9,15,18,19,34−36] Over the past decade, severe air pollution has occurred frequently in China, seriously affecting human health.[10,37,38] Therefore, a better understanding of the chemical composition and reactivity of OA, including the OSs in China, is important. Since OSs in urban areas are highly related to anthropogenic emissions and human activities, OSs formed in different cities present different characteristics.[18] In this study, we have created an "OS precursor map" for OS source identification, which is developed based on the elemental composition information from previous chamber experiments. Then, we compared the chemical composition and possible sources of OSs in ambient $PM_{2.5}$ (particles with aerodynamic diameter $\leq$ 2.5 μm) samples collected in two metropoles, Mainz (a German city within the Rhine-Main region with around a 5.8 million population) and Beijing (a Chinese city with around a 22 million population), where the biogenic/anthropogenic emission and human activities present large differences. An ultrahigh-performance liquid chromatograph (UHPLC) coupled to an Orbitrap mass spectrometer was used for the detailed characterization of OSs at a molecular level. Several synthesized/commercial OS standards, including isoprene/β-pinene/benzene-derived OSs, octyl hydrogen sulfate, and lauryl sulfate, were used as markers to better identify the OSs detected in these ambient samples.

METHODOLOGY

Collection of $PM_{2.5}$ Samples. Six 24-hour integrated Chinese urban $PM_{2.5}$ samples were collected onto prebaked quartz-fiber filters (8 × 10 in., Whatman, QM-A, USA) using a high-volume sampler at a flow rate of 1.05 m^3 min^{-1} during January 7−25, 2014. Similarly, three 24-hour integrated German urban $PM_{2.5}$ samples were collected on borosilicate glass fiber coated with fluorocarbon filters (Ø 70 mm, Pallflex T60A20, Pall Life Science, USA) using a low-volume sampler at a flow rate of 38.3 L min^{-1} from January 14−16, 2015. The sampling site for Chinese samples was located at the urban site of Beijing (39.99° N, 116.39° E) surrounded by residential areas, while the German sampling site was in the campus of Johannes Gutenberg University of Mainz (49.99° N, 8.24° E). According to the daily average $PM_{2.5}$ mass concentration, the $PM_{2.5}$ samples collected in Beijing were divided into two categories for further analysis, Beijing low air pollution level samples with $PM_{2.5}$ mass concentrations lower than 35 μg m^{-3} (referred to as low pollution samples; sample ID, BJL), and Beijing high air pollution samples with $PM_{2.5}$ mass concentrations higher than 150 μg m^{-3} (referred to as high pollution samples; sample ID, BJH). Since the $PM_{2.5}$ mass concentrations in Mainz were all lower than 35 μg m^{-3} during sample collection, we regarded these samples as Mainz low level samples (referred to as low pollution samples; sample ID, MZL). Field blank samples were collected at each site, and all the filter samples were stored at −20 °C until analysis.

The daily ambient meteorological conditions (e.g., temperature; relative humidity; and SO_2, NO_2, CO, and O_3 concentrations) and 48-h backway trajectories of air arriving at the sampling sites during sampling dates are shown in Table S1 and Figure S1, respectively.

Sample Analysis. A portion of the filters (corresponding to about 600 μg particle mass in each extracted filter, 1.05−19.23 cm^2 depending on the $PM_{2.5}$ mass loading) were ultrasonicated for 30 min with an 1.5 mL acetonitrile/ultrapure water (ACN/H_2O) mixture (8/2, v/v). The extraction step was repeated twice with 1 mL of the ACN/H_2O solution. After that, the extracts were combined and filtered through a 0.2 μm polytetrafluoroethylene (PTFE) membrane syringe filter to remove insoluble particulate matter. Then, the extracted solution was evaporated to dryness with a gentle stream of nitrogen at 20 °C. It should be noted, that the evaporation process may accelerate the formation of sulfur/nitrogen-containing compounds with the presence of ammonium sulfate, and/or the pH value is low (~ 2) in the extract solution,[31] resulting in a certain impact on the chemical composition of ambient aerosol samples. Afterward, 1.0 mL of ACN/H_2O (1/9, v/v) was used to redissolve the residue for subsequent analysis.

The chemical identification of OSs was conducted based on ultrahigh-resolution mass spectrometry (UHRMS) using a hybrid-quadrupole-Orbitrap mass spectrometer (Q-Exactive, Thermo Scientific, Germany) coupled to an UHPLC system (Dionex UltiMate 3000, Thermo Scientific, Germany). Analytes were separated by a Hypersil Gold column (C18, 50 × 2.0 mm, 1.9 μm particle size, Thermo Scientific, Germany). The mobile phase consisted of eluent A (ACN with 2% ultrapure H_2O) and eluent B (ultrapure H_2O with 2% ACN and 0.04% formic acid). Gradient elution was optimized at a flow rate of 0.5 mL min^{-1} as follows, 2% A for 1.5 min, a linear increase to 20% A in the next 1 min, 20% A for 3 min, another linear increase to 30% A in 1 min, 30% A for another 1 min, a linear gradient to 50% A in 1 min and immediate increase to 98% A in the next 1 min, 98% A for 2.5 min, back to 2% A in 0.05 min, and then 2% A for 0.05 min. The Orbitrap was equipped with a heated electrospray ionization source (HESI). It was operated in both negative ion mode (ESI−) and positive mode (ESI+) with a −3.3 and +4.0 kV spray voltage, respectively. A mass resolving power of 70 000 @ m/z 200 and a scanning range of 50−500 m/z were applied. The mass spectrometer was externally mass calibrated using a commercial standard calibration solution Ultramark 1621 (Thermo Scientific, Germany) with a mass range of 73−1921 m/z. Each sample extract was analyzed in triplicate with an injection volume of 10.0 μL.

Data Processing. The obtained chromatograms and mass spectra were analyzed by a nontarget screening approach using commercially available software (SIEVE, Thermo Scientific, Germany). A threshold intensity value of 1 × 10^5 arbitrary units in the two-dimensional space of the retention time window from 0.0−11.05 min and m/z from 50 to 500 was applied to all measurements. The software automatically searched peaks above the threshold value, which were significantly different from the background and assigned to the molecular formulas with a mass tolerance of ± 2 ppm. The molecular formulas were presented as $C_cH_hO_oN_nS_s$, where c was the number of carbon atoms in the range of 1−39, h was the number of hydrogen atoms in the range of 1−72, o was the number of oxygen atoms in the range of 0−20, n was the number of nitrogen atoms in the range of 0−7, and s was the number of sulfur atoms in the range of 0−4. In ESI+ mode, 0−

DOI: 10.1021/acs.est.9b02628
Environ. Sci. Technol. 2019, 53, 6192−6202

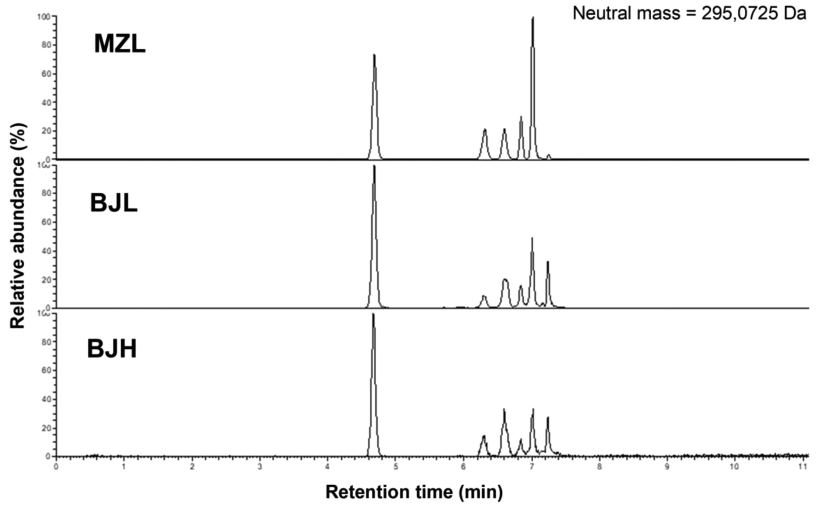

Figure 1. UHPLC chromatograms of tentatively determined $C_{10}H_{17}O_7NS$ (potentially derived from monoterpenes) in Mainz and Beijing samples.

1 of Na atom was considered in the formula assignment. To remove the chemically nonmeaningful molecular formulas, formulas were further constrained by setting H/C, O/C, N/C, and S/C ratios in the ranges of 0.3−3, 0−3, 0−1.3, and 0−0.8, respectively. Meanwhile, the resulting neutral formulas with a noninteger or negative double bond equivalent (DBE) or elemental composition which disobeyed the nitrogen rule for even electron ions were removed. Later, for simplification, we refer to all of the "C", "H", "O", and "S" containing compounds as "CHOS", and all of the "C", "H", "O", "S", and "N" containing compounds as "CHONS".

The DBE value (number of rings plus double bonds) of a molecule reflects the degree of its unsaturation and was calculated by the equation, DBE = $(2c + 2 - h + n)/2$, for the elemental composition $C_cH_hO_oN_nS_s$.

All molar ratios, DBE factors, and molecular formulas presented in this article refer to neutral molecules, and only molecular formulas that are common to all $PM_{2.5}$ samples for each site are considered. The abundance of a compound refers to its chromatographic peak area averaged from all samples in each site. The compounds in samples were compared to those in blanks, and only compounds with a sample-to-blank abundance ratio ≥10 were retained for further data analysis. Subsequently, the abundance of the retained compounds in blanks was subtracted from their abundance in samples.

It should be noted, that the main purpose of this study is to compare the difference of chemical composition and sources of OSs in Mainz and Beijing, so we excluded the OSs with low concentrations through reducing the injection volume from 20.0 μL, in our previous study, to 10 μL, in this study, and increasing the sample-to-blank ratio from 3, in our previous study, to 10, in this study, for data processing, which led to much fewer organic compounds obtained in this study compared to our previous UHRMS study.[11]

RESULTS AND DISCUSSION

Detection of Isomers Using UHPLC Separation. The UHPLC system enables separation of potential isomers which could otherwise be hidden behind a given m/z value. Also, it provides additional information (e.g., retention time), which is helpful for elucidation of the molecular structure of organic compounds. In addition, hundreds of organic compounds can be separated using UHPLC before the ionization process, which can reduce the ion suppression in the ESI source, improving the sensitivity of detection.

Figure 1 illustrates the extracted ion chromatograms for the formula $C_{10}H_{17}O_7NS$, which has been identified as a nitrooxy-OS derived from monoterpenes and has a relatively high abundance compared to other S-containing compounds.[9,15,24,39] As most previous UHRMS studies on OSs mainly used direct infusion,[15,18,40] no isomers with the formula $C_{10}H_{17}O_7NS$ were reported. Compared to three isomers of $C_{10}H_{17}O_7NS$ identified in α/β-pinene-derived chamber experiment by Surratt et al.,[24] in our study, six isomers of $C_{10}H_{17}O_7NS$ were obtained in all samples with varying abundances of each isomer in different sample IDs (see Figure 1), indicating that nitrooxy-OSs are more complex in the ambient atmosphere than in chamber simulations. The abundance of each isomer varies from sample to sample, reflecting the difference in concentrations of corresponding precursors and/or formation mechanisms. In a recent study, Glasius et al.[33] reported the observation of a high concentration of nitrooxy-OS $C_{10}H_{17}O_7NS$ in wintertime aerosol samples in Northern Europe, which was largely impacted by biomass burning emissions, indicating that biomass burning can be an important source for the monoterpene-derived OSs.

The reconstructed Orbitrap mass spectra of CHOS and CHONS compounds observed in Mainz and Beijing samples are shown in Figure S2. Many more molecular formulas related to CHOS and CHONS compounds were detected in Beijing samples than in Mainz samples, indicating the relatively high abundance of S-containing compounds in Beijing OA. This is likely due to much higher SO_2, NO_2, and CO (from incomplete combustion) concentrations (Table S1) in Beijing. Also, in terms of emission sources, a distinct difference between Beijing and Mainz is the large coal combustion emissions from residential heating in Beijing and surrounding areas, which may explain the measurements of more S-containing compounds in Beijing.[37,41] In Beijing samples, 34−57% of CHOS and CHONS compounds contain more than one isomer, while significantly fewer isomers were detected in Mainz samples. This indicates that isomers of organic compounds widely exist in aerosols, especially in the polluted atmosphere, and that S-containing compounds are more

DOI: 10.1021/acs.est.9b02628
Environ. Sci. Technol. 2019, 53, 6192−6202

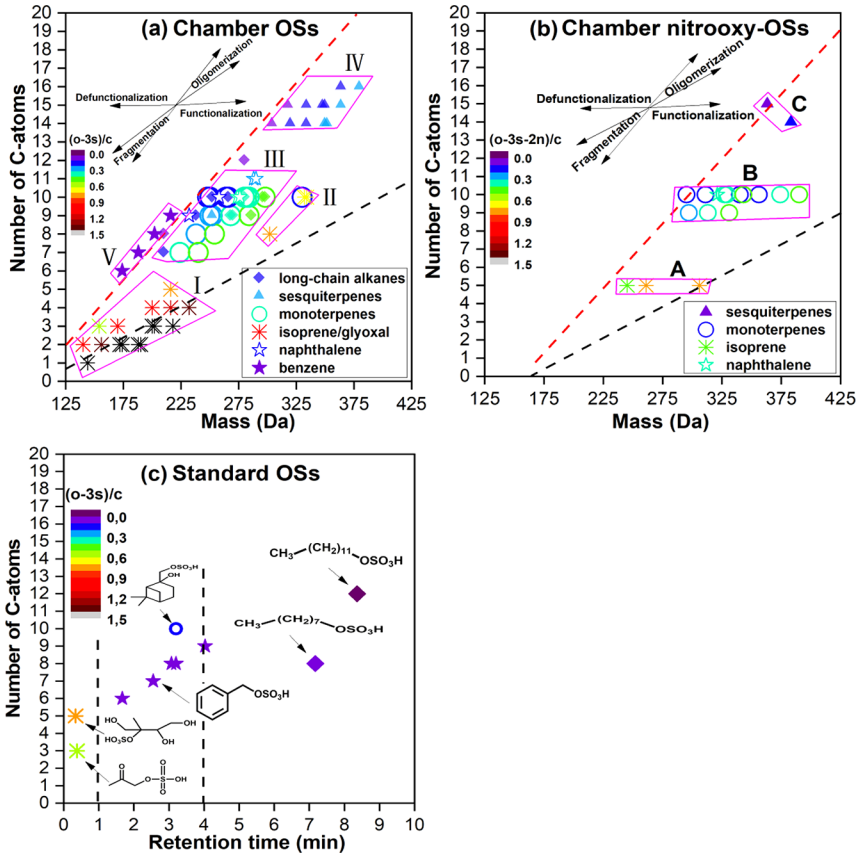

Figure 2. OS precursor map for OSs (a) and nitrooxy-OSs (b) represented by the molar mass and carbon number in the formulas. The dashed lines represent the molecular corridor by linear alkane OSs $C_nH_{2n+1}SO_4$ or nitrooxy-OSs $C_nH_{2n}NO_3SO_4$ (red dashed line) and sugar alcohol OSs $C_nH_{2n+1}O_nSO_4$ or nitrooxy-OSs $C_nH_{2n}O_nNO_3SO_4$ (black dashed line). The regimes marked in roman numbers (I–V) in (a) represent OS derived from isoprene/glyoxal (I), isoprene dimers (II), monoterpenes/long-chain alkenes/naphthalene (III), sesquiterpenes (IV), and benzene (V). The regimes of A, B, and C in (b) represent nitrooxy-OSs derived from isoprene, monoterpenes/naphthalene, and sesquiterpenes, respectively. The vectors correspond to chemical reactions in the atmosphere, including functionalization (addition of polar functional groups, such as hydroxyl), oligomerization (covalent association of two organic precursors), defunctionalization (loss of polar functional groups), and fragmentation (cleavage of C–C bonds). The chromatographic retention time of several standards of OSs together with their structures is shown in (c). It should be noted, that only one molecular structure of benzene-derived Os is shown in (c) due to the similar molecular structures of these five benzene-derived OSs. The color bar indicates the $(o - 3s)/c$ or $(o - 3s - 2n)/c$ ratio.

complex in Beijing than in Mainz, probably due to the highly complex precursors in the Beijing atmosphere.

OS Precursor Map. Several smog chamber experiments have been conducted to understand the formation and chemical composition of OSs and nitrooxy-OSs generated from different precursors.[23,24,27,28,42−44] In this study, we summarized the information (e.g., elemental composition and molecular mass) of previously identified OSs and nitrooxy-OSs (see Table S2) and then created an "OS precursor map" (see Figure 2a,b), which was motivated from Lin et al.'s study in 2012.[15] The "OS precursor map" shows that the experimental data clearly clusters according to precursors and formation pathways, which can thus be used to estimate the precursors of OSs and nitrooxy-OSs in the complex atmospheric aerosol.

Figure 2a,b shows the "OS precursor map" for the OSs and nitrooxy-OSs generated from oxidation of biogenic/anthropogenic precursors, including isoprene/glyoxal, monoterpenes, sesquiterpenes, long-chain alkanes, benzene, and naphthalene. Since glyoxal compounds can be formed from the oxidation of isoprene,[45] we classified precursors of isoprene and glyoxal in one group as isoprene/glyoxal. The color bar in Figure 2 indicates how the oxidized carbon backbone is independent of the sulfate and nitrate groups, which is presented by by $(o - 3s)/c$ and $(o - 3s - 2n)/c$ ratios for OSs and nitrooxy-OSs, respectively. Since the sulfate group and nitrate groups contain three and two more oxygen atoms, respectively, compared to common oxygen-containing groups (e.g., hydroxyl and carbonyl), the use of $(o - 3s)/c$ and $(o - 3s - 2n)/c$ ratios instead of the traditional o/c ratio could better explain the number of additional oxidized groups per carbon atom.

As shown in Figure 2a, the majority of OSs, except several isoprene/glyoxal-derived OSs (asterisk marks in Figure 2a) and the benzene-derived OSs (solid star marks in Figure 2a), fall into a molecular corridor with upper and lower boundaries represented by linear alkane-derived OSs ($C_nH_{2n+1}SO_4$, red dashed line) and sugar alcohol-derived OSs ($C_nH_{2n+1}O_nSO_4$, black dashed line), respectively. Similarly, most nitroxy-OSs are plotted into a molecular corridor with upper and lower boundaries represented by linear alkane-derived nitrooxy-OSs ($C_nH_{2n}NO_3SO_4$, red dashed line) and sugar alcohol nitrooxy-OSs ($C_nH_{2n}O_nNO_3SO_4$, black dashed line). It indicates that this 2-D space of molecular mass and carbon number can constrain most of the OSs and nitrooxy-OSs generated from different precursors. Most isoprene/glyoxal-derived OSs (asterisk marks in Figure 2a) are situated close to the sugar alcohol-derived OSs line in the range of 2–5 carbon numbers

DOI: 10.1021/acs.est.9b02628
Environ. Sci. Technol. 2019, 53, 6192−6202

Table 1. Summary of Formula Number, MM, Elemental Ratios, DBE, and Retention Time (RT) of Compounds Assigned To Be CHOS and CHONS, Which Were Detected in ESI− and ESI+ Modes

sample ID	subgroup	number of formulas[a]	number of formulas with $o/4s$ (or $o/(4s + 3n)$) ≥ 1[b]	MM	H/C	O/C	DBE	RT (min)
MZL	CHOS−	16 (11%)	15 (94%)	212	1.57	1.44	2.81	1.29
	CHONS−	9 (6%)	6 (67%)	297	1.55	0.61	4.33	4.54
	CHONS+	11 (5%)	0 (0%)	247	1.27	0.44	5.55	3.48
BJL	CHOS−	114 (22%)	105 (92%)	212	1.89	0.84	1.46	2.73
	CHONS−	38 (7%)	22 (58%)	265	1.44	0.84	4.55	3.81
	CHONS+	12 (1.4%)	0 (0%)	240	1.28	0.95	4.17	1.57
BJH	CHOS−	86 (15%)	81 (94%)	216	1.57	0.88	2.79	2.40
	CHONS−	36 (6.4%)	14 (39%)	229	1.28	0.95	4.17	1.78
	CHONS+	18 (1.6%)	0 (0%)	235	1.62	0.82	3.50	1.84

[a]Values in parentheses are percentages of CHOS and CHONS formulas among the total number of assigned formulas. [b]Values in parentheses are percentages of CHOS formulas with $o/4s \geq 1$ and CHONS formulas with $o/(4s + 3n) \geq 1$ among the total number of CHOS formulas and CHONS formulas, respectively.

(regime I in Figure 2a) with high $(o - 3s)/c$ ratios ($0.67 \leq (o - 3s)/c$), indicating that they are highly oxidized, and several OSs from isoprene dimers are also reported with carbon numbers exceeding 5 (regime II). As Figure 2a shows, the majority of OSs derived from monoterpenes, long-chain alkanes, and naphthalene have a carbon number of 7−11 (regime III) with an $(o - 3s)/c$ ratio between 0.12 and 0.57, while the sesquiterpene-derived OSs are in the range of 14−16 carbon atoms (regime IV) with an $(o - 3s)/c$ ratio between 0.2 and 0.36. The OSs derived from benzene are located outside of the molecular corridor but close to the linear alkane-derived OSs line in the range of 6−9 carbon numbers (regime V) with a low $(o - 3s)/c$ ratio. Meanwhile, according to the precursors, three different source regimes for nitrooxy-OSs are defined in Figure 2b as follows. Regime A with a carbon number of 5 is dominant with isoprene-derived nitrooxy-OSs; regime B with a carbon number of 9 and 10 is occupied by the nitrooxy-OSs derived from monoterpenes and naphthalene; regime C with a carbon number of 14 and 15 represents the sesquiterpene-derived nitrooxy-OSs.

As the UHPLC technique was applied in this study, the retention time of the standard OS compounds could also be used as additional information to approach the chemical structure properties, such as the polarity. Figure 2c shows the retention time of two synthesized isoprene-derived OSs (isoprene-epoxydiol-derived (IEPOX) OS with the formula $C_5H_{12}O_7S$ and hydroxyacetone OS with the formula $C_3H_6O_5S$); one β-pinene-derived OS with the formula $C_{10}H_{18}O_5S$; five benzene-derived OSs with formulas $C_6H_6O_4S$, $C_7H_8O_4S$, $C_8H_{10}O_4S$ (two isomers), and $C_9H_{12}O_4S$; and two commercial OS standards (lauryl sulfate with the formula $C_{12}H_{26}O_4S$ and octyl hydrogen sulfate with the formula $C_8H_{18}O_4S$). The synthetic procedures for these OS standards are described elsewhere.[19,46] The retention time of the two synthesized isoprene-derived OSs is less than 1 min. Such a short retention time is caused by the polar functional groups hydroxyl and carbonyl in the structure of isoprene-derived OSs, which are quickly eluted from the hydrophobic C18 column. The synthesized β-pinene-derived OS and five benzene-derived OSs have retention times between 1 and 4 min, indicating that fewer polar functional groups exist in their chemical structures compared to isoprene-derived OSs. The two commercially available long-chain alkane-derived OSs have the longest retention times (> 4 min) compared to the other OSs, due to the strong adsorption of the long alkyl chain in these OSs to the hydrophobic C18 column.

Though the OSs and nitrooxy-OSs observed in chamber simulations cannot cover all the OSs and nitrooxy-OSs in atmospheric OA, the "OS precursor map" and the retention time of OS standards in Figure 2 can be used to estimate the precursors of OSs and nitrooxy-OSs in atmospheric OA and to better understand their molecular structures and properties. It should be noted, that the "OS precursor map" is created from chamber results of fresh aerosols without considering atmospheric aging. The most important aging process to be considered for these compounds will be oxidative processing. Although the oxidation can also take place in the condensed phase (e.g., heterogeneous and aqueous-phase oxidation) and certainly cannot be excluded here, the gas-phase oxidation is a more important oxidative aging process for most organic compounds because heterogeneous oxidation mechanisms appear to be incapable of oxidizing OA with sufficient speed, while gas-phase oxidation can do so.[47,48] However, the low volatility of OSs will keep them in the particle-phase, and therefore, the gas-phase oxidative aging is very likely not important for OSs. The other aging pathways, including oligomerization and photolysis, might play a role, as shown in the "OS precursor map" with vectors, but these are largely unknown.

Comparison of CHOS in Mainz and Beijing Aerosol Samples. Table 1 summarizes the averaged characteristics (molecular mass (MM), elemental ratios, retention time, and DBE) of assigned CHOS and CHONS compounds. Compounds with a number of oxygen atoms greater than or equal to four were tentatively regarded as OSs.[9,15] However, tandem MS experiments were not conducted on the S-containing ions detected in these samples, and therefore, other S-containing compounds, such as sulfonates, may also be assigned to this group. As many as 15−22% of organic compounds in Beijing samples were identified as CHOS compounds, while the fraction decreases to 11% in Mainz samples (Table 1). The majority (92−94%) of CHOS formulas in both Mainz and Beijing samples were assigned with $o/4s \geqslant 1$, suggesting that these compounds are OSs, which is consistent with previous studies.[9,15,18] The averaged O/C of CHOS compounds in Mainz samples is 1.44, which is significantly higher than that in Beijing samples (0.84 in BJL and 0.88 in BJH), indicating a higher oxidation state of OSs in Mainz OA.

To estimate the precursors of OSs observed in Mainz and Beijing samples, the "OS precursor map" was applied in Figure 3a−c. The majority of OSs in both Mainz and Beijing samples

DOI: 10.1021/acs.est.9b02628
Environ. Sci. Technol. 2019, 53, 6192−6202

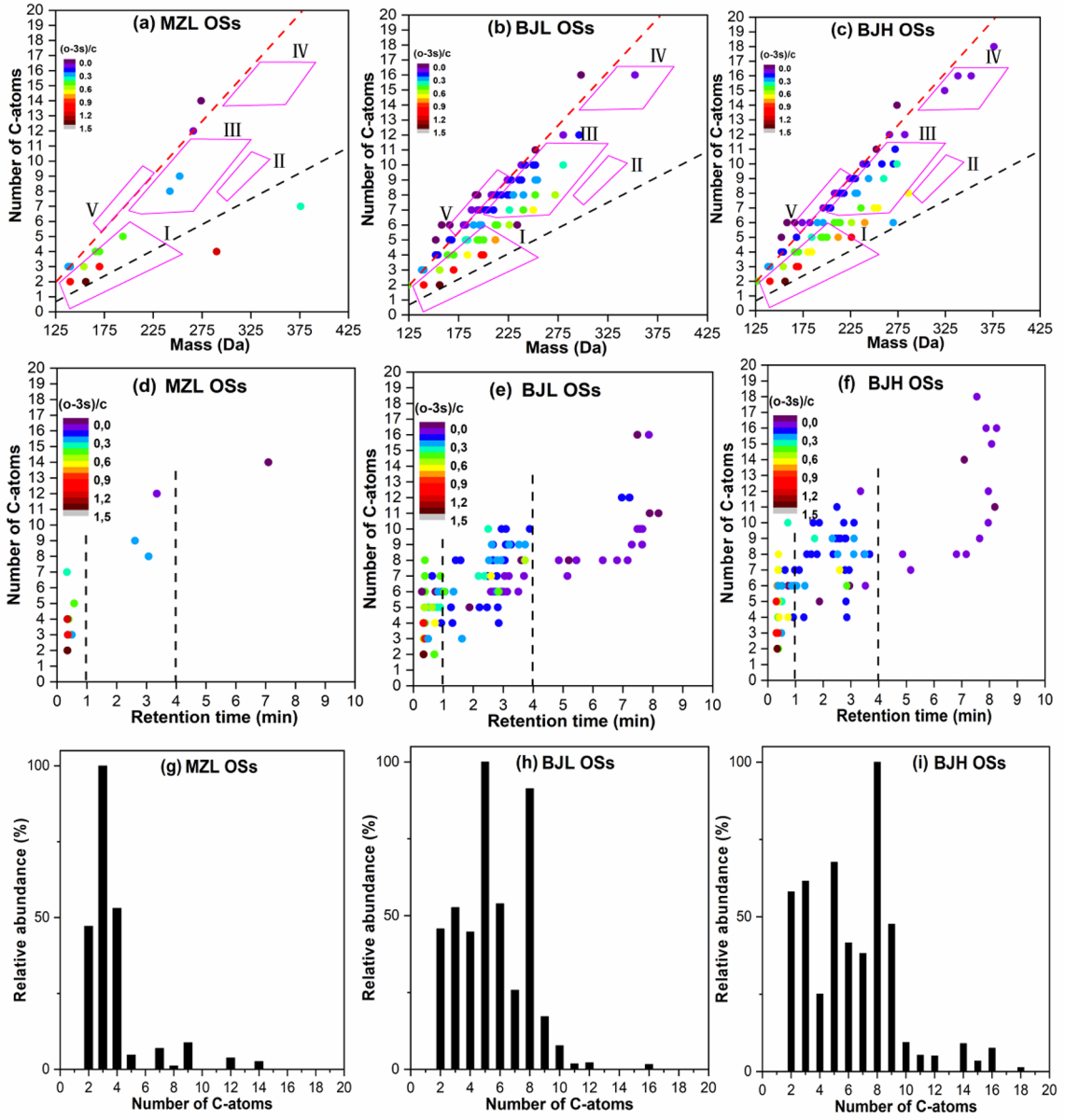

Figure 3. (a–c) The "OS precursor map" applied to OSs detected in Mainz and Beijing aerosol samples. (d–f) The retention time of OSs in Mainz and Beijing samples. (g–i) The relative abundance distribution of OSs in Mainz and Beijing samples.

fall into the molecular corridor represented by linear alkane OSs and sugar alcohol OSs, indicating that the 2-D space of molar mass and carbon number can constrain not only the chamber OSs but also the complex atmospheric aerosol OSs. As shown in Figure 3a, most OSs in Mainz samples are located in regime I in a range of carbon numbers 2–5 with a high $(o - 3s)/c$ ratio, indicating that OSs in Mainz were mainly derived from isoprene/glyoxal or other unknown precursors with small carbon atoms.[33,49] However, the OSs observed in Beijing samples cover almost all regimes of I–V (except regime II) with carbon numbers of 2–16 (see Figure 3b,c), and OSs in regime I (represented by isoprene/glyoxal-derived OSs) and regime III (represented by monoterpenes, long-chain alkane- and naphthalene-derived OSs) are dominant, indicating the highly complex precursors in Beijing. The dominance of isoprene-derived OSs in winter is not surprising because of increasing evidence showing that isoprene is very likely from biomass burning emissions. For example, a recent study from Glasius et al.[33] identified and quantified a group of OSs originated from the photochemical oxidation of isoprene during winter in six Northern European sites, accounting for 13 ± 5% of the sum of measured OSs. Biomass burning emissions were suggested to be the source of isoprene during winter in this study. Ding et al.[50] also showed that a considerable fraction (10–30 ng m^{-3}) of isoprene-derived SOA in wintertime samples in 12 Chinese sites, including Beijing, was related to biomass burning emissions. In terms of atmospheric oxidative capacity, we note, that wintertime photochemistry was traditionally thought to be low because the wintertime OH radical concentrations were traditionally thought to be low due to low O_3 concentrations and the reduced photolysis of O_3 due to the low UV-B levels during winter. However, recent OH radical measurements by Tan et al.[51] using a laser-induced fluorescence (LIF) system at a suburban site near Beijing from January to March 2016 reported OH radical concentrations at noontime ranged from

DOI: 10.1021/acs.est.9b02628
Environ. Sci. Technol. 2019, 53, 6192–6202

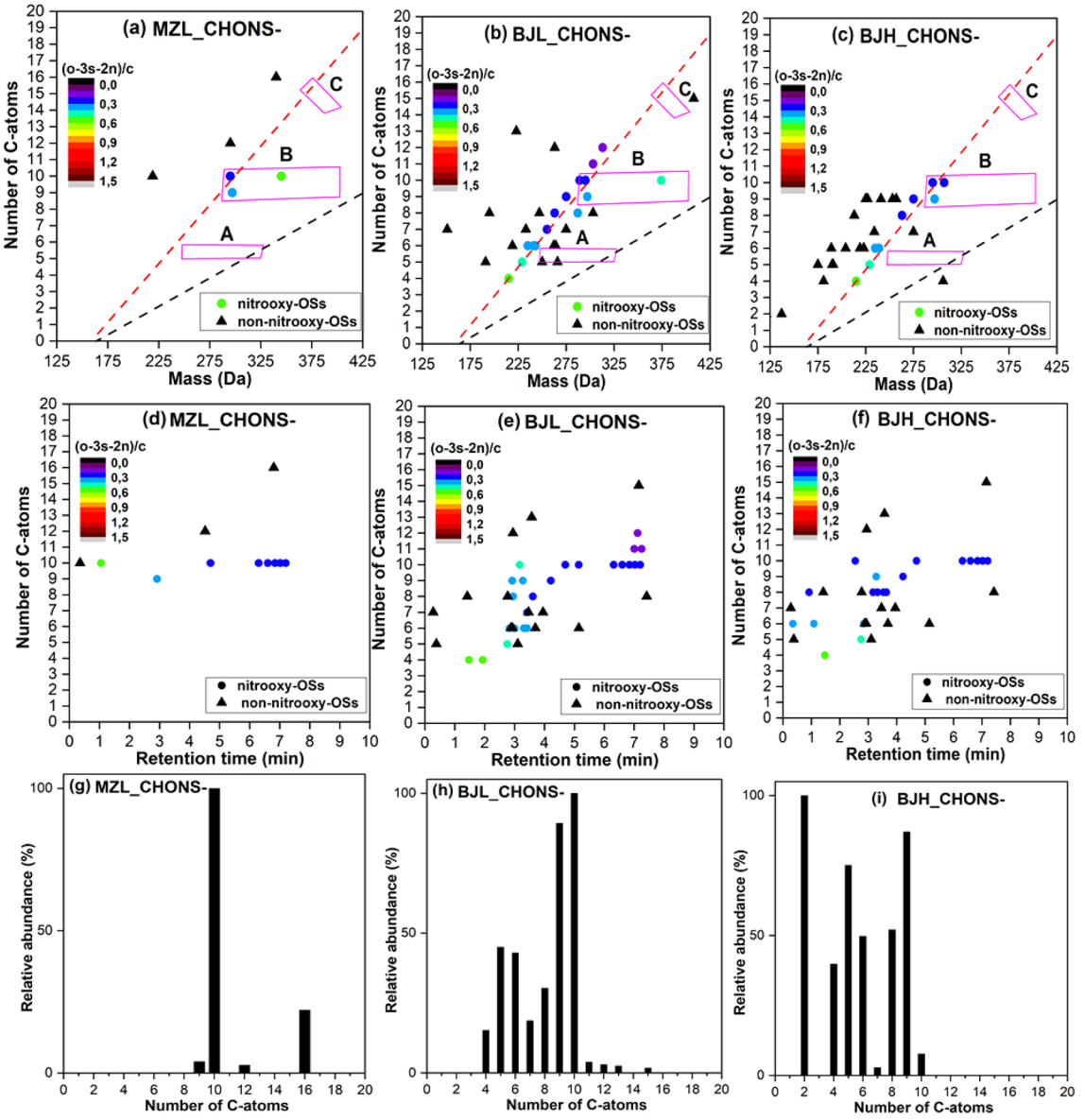

Figure 4. (a–c) The "OS precursor map" applied on CHONS compounds in Mainz and Beijing aerosol samples. (d–f) The retention time of CHONS. (g–i) The relative abundance distribution of CHONS in Mainz and Beijing samples.

2.4×10^6 cm^{-3} in severely polluted air ($k_{OH} \sim 27$ s^{-1}) to 3.6×10^6 cm^{-3} in relatively clean air ($k_{OH} \sim 5$ s^{-1}). These values are nearly 2-fold larger than OH concentrations observed in previous winter campaigns in Birmingham, Tokyo, and New York City but similar to those observed at a rural site in Colorado in late February (up to 2.7×10^6 cm^{-3}).[51,52] The observed OH concentrations are nearly 1 order of magnitude larger than what global models predict for northern China in winter.[53] The higher-than-expected OH concentrations and moderate OH reactivity in Beijing and in the North China Plain resulted in a fast oxidation rate, even in winter, explaining the high contribution of SOA during wintertime severe haze events.[37] Note, that increasing evidence shows that HONO, instead of O_3, is the main source of OH radicals in the wintertime North China Plain.[54,55] Further, glyoxal- and methylglyoxal-derived SOA are found to constitute 8.5–30.2% of the observed SOA during the same measurement campaign of our study in Beijing, indicating that glyoxal-related compounds (e.g., glyoxal, glycolaldehyde and glycolic acid) could also be a source for OSs with a carbon atom number $\leqslant 5$ located in regime I in the "OS precursor map". The OS formation from glyoxal and glycolaldehyde has been reported in previous studies by Lim et al.[44] and Perri et al.[43]

Figure 3d–f shows the retention time of OSs in the UHPLC system, which is affected by their polarity and hydrophobicity. The majority of OSs from Mainz samples have retention times below 1 min with a high $(o - 3s)/c$ ratio and 2–7 carbon numbers (Figure 3d), further indicating that they are mostly isoprene/glyoxal-derived or from other small precursors. However, the OSs in Beijing samples show a broad range of retention times between 0 and 9 min (Figure 3e,f). As discussed above, OSs with retention times of 0–1 min are probably derived from isoprene/glyoxal or other small polar molecules;[33,49] OSs with retention times of 1–4 min are likely derived from monoterpenes, benzene, and naphthalene; while OSs with retention times of 4–9 min are probably derived from long-chain alkanes and sesquiterpenes. The broad range of retention times additionally illustrates that OSs in Beijing

DOI: 10.1021/acs.est.9b02628
Environ. Sci. Technol. 2019, 53, 6192–6202

aerosol were generated from both biogenic and anthropogenic precursors.

On the basis of the carbon numbers, Figure 3g–i presents the relative abundance of OSs. In Mainz aerosol samples, C_3–OSs are dominant, which is suggested to be hydroxyacetone sulfate originating from photochemical oxidation of isoprene or combustion emissions (e.g., biomass burning and fossil fuel combustion).[19,49] However, C_5–OSs and C_8–OSs show the maximum relative abundances in BJL and BJH samples, respectively. The C_5–OSs are probably related to isoprene-derived OSs, and C_8–OSs are likely related to aromatic OSs.[27] Moreover, OSs with a high carbon number ($C \geq 10$) in BJH samples have a significantly higher abundance compared to those in MZL and BJL samples. This indicates that, in polluted air, more OSs are generated from long-chain alkanes, which is consistent with Tao et al.'s study showing that the molecular structures of OSs collected in Shanghai contain longer carbon chains than those collected in Los Angeles.[18]

Comparison of CHONS in Mainz and Beijing Aerosol Samples. As shown in Table 1, 9–38 CHONS compounds were observed in Mainz and Beijing aerosol samples. These compounds have a higher average MM (235–297 Da) compared to CHOS compounds due to the presence of one or two additional nitrate groups.[10] In the ESI– mode, 58–67% of CHONS– in Mainz and BJL samples contain enough oxygen atoms to allow for the assignment of $-OSO_3H$ and $-ONO_2$ groups ($o/(4s + 3n) \geqslant 1$) in their formulas, indicating that they are nitrooxy-OSs.[9,15] However, only 39% of CHONS– compounds were assigned as nitrooxy-OSs in BJH samples, showing the large difference in chemical composition of CHONS– compounds in the clean and polluted air.

Figure 4 shows the application of the "OS precursor map" on the CHONS– compounds observed in Mainz and Beijing samples. As shown in Figure 4a–c, no nitrooxy-OSs are observed in regimes A and C, indicating that no isoprene or sesquiterpene-derived nitrooxy-OSs were detected. A few nitrooxy-OSs plots are located in the regime B, suggesting that they were probably generated from monoterpenes or naphthalene precursors. In Beijing samples, many nitrooxy-OSs are found outside of the molecular corridor but close to the linear alkane-derived nitrooxy-OSs line, indicating that the precursors of these nitrooxy-OSs are similar to linear alkanes but more unsaturated. Meanwhile, several non-nitrooxy-OS CHONS– compounds were also identified. These non-nitrooxy-OS CHONS– compounds probably contain one amino or sulfhydryl group, which are less oxidized, and they are present in larger numbers in the polluted Beijing sample compared to the Mainz and clean Beijing samples.

The diagrams of carbon number plotted by retention time in Figure 4d–f show that CHONS– compounds in both the Mainz and Beijing aerosol samples cover a broad retention time range between 0 and 9 min. However, more CHONS– compounds with retention times less than 4 min were detected in Beijing samples (see Figure 4e,f), showing that more polar functional groups (e.g., hydroxyl group) were present in the Beijing CHONS– compounds. This observation is consistent with the results in Table 1 showing that higher O/C ratios of CHONS– are observed in Beijing samples compared to Mainz samples. However, the O/C ratios of CHOS in Beijing samples are lower than those in Mainz samples, indicating differences in the formation efficiency and mechanisms of CHOS and CHONS compounds.

The relative abundance of each subgroup of CHONS– compounds based on the carbon number is shown in Figure 4g–i. The CHONS– compounds with a carbon number of 10 (e.g., $C_{10}H_{17}O_7NS$) are dominant in Mainz and BJL samples, indicating that monoterpenes are the most important nitrooxy-OS precursors for clean-day OA. However, in BJH samples, the CHONS– compound with a molecular formula of $C_2H_3O_4NS$ shows the maximum abundance, which could be assigned a cyano group-containing OS, indicating the different precursors for CHONS– compounds between clean-day and pollution-day OA.

Implications. This work shows that the "OS precursor map" developed here for OSs and nitrooxy-OSs, together with the polarity information provided by UHPLC, can provide important information on possible precursors and chemical properties of these compounds and will be useful in future studies of their formation and occurrence. Meanwhile, additional information on elemental composition of OSs and nitrooxy-OSs identified in future chamber simulations can be used to further improve this "OS precursor map". In addition, a large amount of isoprene-derived OSs were identified in aerosol samples during wintertime in this study, and biomass burning was suggested to be the important source of isoprene, indicating that the contribution of isoprene to SOA in winter might be more important than traditionally expected.

■ ASSOCIATED CONTENT

Supporting Information

The Supporting Information is available free of charge on the ACS Publications website at DOI: 10.1021/acs.est.9b02628.

The ambient meteorologic conditions in the sites during sampling dates, list of the molecular formulas of OSs and nitrooxy-OSs generated from chamber experiments, back trajectories of air arriving to the sampling sites, and the Orbitrap mass spectra of CHOS and CHONS compounds detected in Mainz and Beijing aerosol samples (PDF)

■ AUTHOR INFORMATION

Corresponding Author

*E-mail: rujin.huang@ieecas.cn.

ORCID

Ru-Jin Huang: 0000-0002-4907-9616

Marianne Glasius: 0000-0002-4404-6989

Notes

The authors declare no competing financial interest.

■ ACKNOWLEDGMENTS

This study was supported by the National Natural Science Foundation of China (NSFC, Grant 41877408 and 91644219), the National Key Research and Development Program of China (2017YFC0212701), and the German Research Foundation (Deutsche Forschungsgemeinschaft, DFG) under Grant INST 247/664-1 FUGG. K.W. acknowledges the scholarship from the Chinese Scholarship Council (CSC) and Max Plank Graduate Center with Johannes Gutenberg University of Mainz (MPGC) and thanks Prof. Ulrich Pöschl for his helpful suggestion on this study.

DOI: 10.1021/acs.est.9b02628
Environ. Sci. Technol. 2019, 53, 6192–6202

REFERENCES

(1) Jimenez, J. L.; Canagaratna, M. R.; Donahue, N. M.; Prevot, A. S. H.; Zhang, Q.; Kroll, J. H.; DeCarlo, P. F.; Allan, J. D.; Coe, H.; Ng, N. L.; Aiken, A. C.; Docherty, K. S.; Ulbrich, I. M.; Grieshop, A. P.; Robinson, A. L.; Duplissy, J.; Smith, J. D.; Wilson, K. R.; Lanz, V. A.; Hueglin, C.; Sun, Y. L.; Tian, J.; Laaksonen, A.; Raatikainen, T.; Rautiainen, J.; Vaattovaara, P.; Ehn, M.; Kulmala, M.; Tomlinson, J. M.; Collins, D. R.; Cubison, M. J.; Dunlea, E. J.; Huffman, J. A.; Onasch, T. B.; Alfarra, M. R.; Williams, P. I.; Bower, K.; Kondo, Y.; Schneider, J.; Drewnick, F.; Borrmann, S.; Weimer, S.; Demerjian, K.; Salcedo, D.; Cottrell, L.; Griffin, R.; Takami, A.; Miyoshi, T.; Hatakeyama, S.; Shimono, A.; Sun, J. Y.; Zhang, Y. M.; Dzepina, K.; Kimmel, J. R.; Sueper, D.; Jayne, J. T.; Herndon, S. C.; Trimborn, A. M.; Williams, L. R.; Wood, E. C.; Middlebrook, A. M.; Kolb, C. E.; Baltensperger, U.; Worsnop, D. R. Evolution of Organic Aerosols in the Atmosphere. *Science* **2009**, *326* (5959), 1525−1529.

(2) Kroll, J. H.; Donahue, N. M.; Jimenez, J. L.; Kessler, S. H.; Canagaratna, M. R.; Wilson, K. R.; Altieri, K. E.; Mazzoleni, L. R.; Wozniak, A. S.; Bluhm, H.; Mysak, E. R.; Smith, J. D.; Kolb, C. E.; Worsnop, D. R. Carbon oxidation state as a metric for describing the chemistry of atmospheric organic aerosol. *Nat. Chem.* **2011**, *3* (2), 133−139.

(3) Pöschl, U. Atmospheric aerosols: composition, transformation, climate and health effects. *Angew. Chem., Int. Ed.* **2005**, *44* (46), 7520−7540.

(4) Hallquist, M.; Wenger, J. C.; Baltensperger, U.; Rudich, Y.; Simpson, D.; Claeys, M.; Dommen, J.; Donahue, N. M.; George, C.; Goldstein, A. H.; Hamilton, J. F.; Herrmann, H.; Hoffmann, T.; Iinuma, Y.; Jang, M.; Jenkin, M. E.; Jimenez, J. L.; Kiendler-Scharr, A.; Maenhaut, W.; McFiggans, G.; Mentel, T. F.; Monod, A.; Prevot, A. S. H.; Seinfeld, J. H.; Surratt, J. D.; Szmigielski, R.; Wildt, J. The formation, properties and impact of secondary organic aerosol: current and emerging issues. *Atmos. Chem. Phys.* **2009**, *9* (14), 5155−5236.

(5) Pöschl, U.; Shiraiwa, M. Multiphase chemistry at the atmosphere-biosphere interface influencing climate and public health in the anthropocene. *Chem. Rev.* **2015**, *115* (10), 4440−75.

(6) Schum, S. K.; Zhang, B.; Džepina, K.; Fialho, P.; Mazzoleni, C.; Mazzoleni, L. R. Molecular and physical characteristics of aerosol at a remote free troposphere site: implications for atmospheric aging. *Atmos. Chem. Phys.* **2018**, *18* (19), 14017−14036.

(7) Seinfeld, J. H.; Pankow, J. F. Organic atmospheric particulate material. *Annu. Rev. Phys. Chem.* **2003**, *54*, 121−40.

(8) Glasius, M.; Goldstein, A. H. Recent Discoveries and Future Challenges in Atmospheric Organic Chemistry. *Environ. Sci. Technol.* **2016**, *50* (6), 2754−2764.

(9) Wang, X. K.; Rossignol, S.; Ma, Y.; Yao, L.; Wang, M. Y.; Chen, J. M.; George, C.; Wang, L. Molecular characterization of atmospheric particulate organosulfates in three megacities at the middle and lower reaches of the Yangtze River. *Atmos. Chem. Phys.* **2016**, *16* (4), 2285−2298.

(10) Wang, X. K.; Hayeck, N.; Brüggemann, M.; Yao, L.; Chen, H. F.; Zhang, C.; Emmelin, C.; Chen, J. M.; George, C.; Wang, L. Chemical characterization of organic aerosol in: A study by Ultrahigh-Performance Liquid Chromatography Coupled with Orbitrap Mass Spectrometry. *Journal of Geophysical Research-Atmospheres* **2017**, *122* (21), 703−722.

(11) Wang, K.; Zhang, Y.; Huang, R.-J.; Cao, J.; Hoffmann, T. UHPLC-Orbitrap mass spectrometric characterization of organic aerosol from a central European city (Mainz, Germany) and a Chinese megacity (Beijing). *Atmos. Environ.* **2018**, *189*, 22−29.

(12) Zhao, Y.; Hallar, A. G.; Mazzoleni, L. R. Atmospheric organic matter in clouds: exact masses and molecular formula identification using ultrahigh-resolution FT-ICR mass spectrometry. *Atmos. Chem. Phys.* **2013**, *13* (24), 12343−12362.

(13) Iinuma, Y.; Müller, C.; Berndt, T.; Böge, O.; Claeys, M.; Herrmann, H. Evidence for the existence of organosulfates from β-pinene ozonolysis in ambient secondary organic aerosol. *Environ. Sci. Technol.* **2007**, *41*, 6678−6683.

(14) Kristensen, K.; Glasius, M. Organosulfates and oxidation products from biogenic hydrocarbons in fine aerosols from a forest in North West Europe during spring. *Atmos. Environ.* **2011**, *45* (27), 4546−4556.

(15) Lin, P.; Yu, J. Z.; Engling, G.; Kalberer, M. Organosulfates in humic-like substance fraction isolated from aerosols at seven locations in East Asia: a study by ultra-high-resolution mass spectrometry. *Environ. Sci. Technol.* **2012**, *46* (24), 13118−27.

(16) Lin, Y. H.; Budisulistiorini, S. H.; Chu, K.; Siejack, R. A.; Zhang, H.; Riva, M.; Zhang, Z.; Gold, A.; Kautzman, K. E.; Surratt, J. D. Light-absorbing oligomer formation in secondary organic aerosol from reactive uptake of isoprene epoxydiols. *Environ. Sci. Technol.* **2014**, *48* (20), 12012−21.

(17) Nguyen, Q. T.; Christensen, M. K.; Cozzi, F.; Zare, A.; Hansen, A. M. K.; Kristensen, K.; Tulinius, T. E.; Madsen, H. H.; Christensen, J. H.; Brandt, J.; Massling, A.; Noejgaard, J. K.; Glasius, M. Understanding the anthropogenic influence on formation of biogenic secondary organic aerosols in Denmark via analysis of organosulfates and related oxidation products. *Atmos. Chem. Phys.* **2014**, *14* (17), 8961−8981.

(18) Tao, S.; Lu, X.; Levac, N.; Bateman, A. P.; Nguyen, T. B.; Bones, D. L.; Nizkorodov, S. A.; Laskin, J.; Laskin, A.; Yang, X. Molecular Characterization of Organosulfates in Organic Aerosols from Shanghai and Los Angeles Urban Areas by Nanospray-Desorption Electrospray Ionization High-Resolution Mass Spectrometry. *Environ. Sci. Technol.* **2014**, *48* (18), 10993−11001.

(19) Huang, R. J.; Cao, J.; Chen, Y.; Yang, L.; Shen, J.; You, Q.; Wang, K.; Lin, C.; Xu, W.; Gao, B.; Li, Y.; Chen, Q.; Hoffmann, T.; O'Dowd, C. D.; Bilde, M.; Glasius, M. Organosulfates in atmospheric aerosol: synthesis and quantitative analysis of PM2.5 from Xi'an, northwestern China. *Atmos. Mea. Atmos. Meas. Tech.* **2018**, *11* (6), 3447−3456.

(20) Wang, Y.; Ren, J.; Huang, X. H. H.; Tong, R.; Yu, J. Z. Synthesis of Four Monoterpene-Derived Organosulfates and Their Quantification in Atmospheric Aerosol Samples. *Environ. Sci. Technol.* **2017**, *51* (12), 6791−6801.

(21) Kuang, B. Y.; Lin, P.; Hu, M.; Yu, J. Z. Aerosol size distribution characteristics of organosulfates in the Pearl River Delta region, China. *Atmos. Environ.* **2016**, *130*, 23−35.

(22) Hansen, A. M. K.; Hong, J.; Raatikainen, T.; Kristensen, K.; Ylisirniö, A.; Virtanen, A.; Petäjä, T.; Glasius, M.; Prisle, N. L. Hygroscopic properties and cloud condensation nuclei activation of limonene-derived organosulfates and their mixtures with ammonium sulfate. *Atmos. Chem. Phys.* **2015**, *15* (24), 14071−14089.

(23) Surratt, J. D.; Kroll, J. H.; Edney, E. O.; Sorooshian, A.; Ng, N. L.; Kleindienst, T. E.; Jaoui, M.; Offenberg, J. H.; Claeys, M.; Flagan, R. C.; Seinfeld, J. H.; Lewandowski, M. Evidence for Organosulfate in Secondary Organic Aerosol. *Environ. Sci. Technol.* **2007**, *41*, 517−527.

(24) Surratt, J. D.; Gómez-González, Y.; Chan, A. W.; Vermeylen, R.; Shahgholi, M.; Kleindienst, T. E.; Edney, E. O.; Offenberg, J. H.; Lewandowski, M.; Jaoui, M.; Maenhaut, W.; Claeys, M.; Flagan, R. C.; Seinfeld, J. H. Organosulfate Formation in Biogenic Secondary Organic Aerosol. *J. Phys. Chem. A* **2008**, *112*, 8345−8378.

(25) Ng, N. L.; Kwan, A. J.; Surratt, J. D.; Chan, A. W.; Chhabra, P. S.; Sorooshian, A.; Pye, H. O. T.; Crounse, J. D.; Wennberg, P. O.; Flagan, R. C.; Seinfeld, J. H. Secondary organic aerosol (SOA) fromation from reaction of isoprene with nitrate radicals (NO3). *Atmos. Chem. Phys.* **2008**, *8*, 4117−4140.

(26) Iinuma, Y.; Böge, O.; Kahnt, A.; Herrmann, H. Laboratory chamber studies on the formation of organosulfates from reactive uptake of monoterpene oxides. *Phys. Chem. Chem. Phys.* **2009**, *11*, 7985−7997.

(27) Riva, M.; Tomaz, S.; Cui, T.; Lin, Y.-H.; Perraudin, E.; Gold, A.; Stone, E. A.; Villenave, E.; Surratt, J. D. Evidence for an Unrecognized Secondary Anthropogenic Source of Organosulfates and Sulfonates: Gas-Phase Oxidation of Polycyclic Aromatic Hydrocarbons in the Presence of Sulfate Aerosol. *Environ. Sci. Technol.* **2015**, *49* (11), 6654−6664.

DOI: 10.1021/acs.est.9b02628
Environ. Sci. Technol. 2019, 53, 6192−6202

(28) Riva, M.; Da Silva Barbosa, T.; Lin, Y.-H.; Stone, E. A.; Gold, A.; Surratt, J. D. Chemical characterization of organosulfates in secondary organic aerosol derived from the photooxidation of alkanes. *Atmos. Chem. Phys.* **2016**, *16* (17), 11001−11018.
(29) Shalamzari, M. S.; Vermeylen, R.; Blockhuys, F.; Kleindienst, T. E.; Lewandowski, M.; Szmigielski, R.; Rudzinski, K. J.; Spólnik, G.; Danikiewicz, W.; Maenhaut, W.; Claeys, M. Characterization of polar organosulfates in secondary organic aerosol from the unsaturated aldehydes 2-E-pentenal, 2-E-hexenal, and 3-Z-hexenal. *Atmos. Chem. Phys.* **2016**, *16* (11), 7135−7148.
(30) Martinsson, J.; Monteil, G.; Sporre, M. K.; Kaldal Hansen, A. M.; Kristensson, A.; Eriksson Stenström, K.; Swietlicki, E.; Glasius, M. Exploring sources of biogenic secondary organic aerosol compounds using chemical analysis and the FLEXPART model. *Atmos. Chem. Phys.* **2017**, *17* (18), 11025−11040.
(31) Nguyen, T. B.; Lee, P. B.; Updyke, K. M.; Bones, D. L.; Laskin, J.; Laskin, A.; Nizkorodov, S. A. Formation of nitrogen- and sulfur-containing light-absorbing compounds accelerated by evaporation of water from secondary organic aerosols. *Journal of Geophysical Research-Atmospheres* **2012**, *117*, D01207.
(32) Worton, D. R.; Goldstein, A. H.; Farmer, D. K.; Docherty, K. S.; Jimenez, J. L.; Gilman, J. B.; Kuster, W. C.; de Gouw, J.; Williams, B. J.; Kreisberg, N. M.; Hering, S. V.; Bench, G.; McKay, M.; Kristensen, K.; Glasius, M.; Surratt, J. D.; Seinfeld, J. H. Origins and composition of fine atmospheric carbonaceous aerosol in the Sierra Nevada Mountains, California. *Atmos. Chem. Phys.* **2011**, *11* (19), 10219−10241.
(33) Glasius, M.; Hansen, A. M. K.; Claeys, M.; Henzing, J. S.; Jedynska, A. D.; Kasper-Giebl, A.; Kistler, M.; Kristensen, K.; Martinsson, J.; Maenhaut, W.; Nøjgaard, J. K.; Spindler, G.; Stenström, K. E.; Swietlicki, E.; Szidat, S.; Simpson, D.; Yttri, K. E. Composition and sources of carbonaceous aerosols in Northern Europe during winter. *Atmos. Environ.* **2018**, *173*, 127−141.
(34) He, Q. F.; Ding, X.; Wang, X. M.; Yu, J. Z.; Fu, X. X.; Liu, T. Y.; Zhang, Z.; Xue, J.; Chen, D. H.; Zhong, L. J.; Donahue, N. M. Organosulfates from pinene and isoprene over the Pearl River Delta, South China: seasonal variation and implication in formation mechanisms. *Environ. Sci. Technol.* **2014**, *48* (16), 9236−45.
(35) Ma, Y.; Xu, X.; Song, W.; Geng, F.; Wang, L. Seasonal and diurnal variations of particulate organosulfates in urban Shanghai, China. *Atmos. Environ.* **2014**, *85*, 152−160.
(36) Le Breton, M.; Wang, Y.; Hallquist, Å. M.; Pathak, R. K.; Zheng, J.; Yang, Y.; Shang, D.; Glasius, M.; Bannan, T. J.; Liu, Q.; Chan, C. K.; Percival, C. J.; Zhu, W.; Lou, S.; Topping, D.; Wang, Y.; Yu, J.; Lu, K.; Guo, S.; Hu, M.; Hallquist, M. Online gas- and particle-phase measurements of organosulfates, organosulfonates and nitrooxy organosulfates in Beijing utilizing a FIGAERO ToF-CIMS. *Atmos. Chem. Phys.* **2018**, *18* (14), 10355−10371.
(37) Huang, R. J.; Zhang, Y.; Bozzetti, C.; Ho, K. F.; Cao, J. J.; Han, Y.; Daellenbach, K. R.; Slowik, J. G.; Platt, S. M.; Canonaco, F.; Zotter, P.; Wolf, R.; Pieber, S. M.; Bruns, E. A.; Crippa, M.; Ciarelli, G.; Piazzalunga, A.; Schwikowski, M.; Abbaszade, G.; Schnelle-Kreis, J.; Zimmermann, R.; An, Z.; Szidat, S.; Baltensperger, U.; El Haddad, I.; Prevot, A. S. High secondary aerosol contribution to particulate pollution during haze events in China. *Nature* **2014**, *514* (7521), 218−22.
(38) Jiang, B.; Kuang, B. Y.; Liang, Y.; Zhang, J.; Huang, X. H. H.; Xu, C.; Yu, J. Z.; Shi, Q. Molecular composition of urban organic aerosols on clear and hazy days in Beijing: a comparative study using FT-ICR MS. *Environ. Chem.* **2016**, *13* (5), 888.
(39) Brüggemann, M.; Poulain, L.; Held, A.; Stelzer, T.; Zuth, C.; Richters, S.; Mutzel, A.; van Pinxteren, D.; Iinuma, Y.; Katkevica, S.; Rabe, R.; Herrmann, H.; Hoffmann, T. Real-time detection of highly oxidized organosulfates and BSOA marker compounds during the F-BEACh 2014 field study. *Atmos. Chem. Phys.* **2017**, *17* (2), 1453−1469.
(40) Kourtchev, I.; Godoi, R. H. M.; Connors, S.; Levine, J. G.; Archibald, A. T.; Godoi, A. F. L.; Paralovo, S. L.; Barbosa, C. G. G.; Souza, R. A. F.; Manzi, A. O.; Seco, R.; Sjostedt, S.; Park, J.-H.; Guenther, A.; Kim, S.; Smith, J.; Martin, S. T.; Kalberer, M. Molecular composition of organic aerosols in central Amazonia: an ultra-high-resolution mass spectrometry study. *Atmos. Chem. Phys.* **2016**, *16* (18), 11899−11913.
(41) Song, J.; Li, M.; Jiang, B.; Wei, S.; Fan, X.; Peng, P. Molecular Characterization of Water-Soluble Humic like Substances in Smoke Particles Emitted from Combustion of Biomass Materials and Coal Using Ultrahigh-Resolution Electrospray Ionization Fourier Transform Ion Cyclotron Resonance Mass Spectrometry. *Environ. Sci. Technol.* **2018**, *52* (5), 2575−2585.
(42) Chan, M. N.; Surratt, J. D.; Chan, A. W. H.; Schilling, K.; Offenberg, J. H.; Lewandowski, M.; Edney, E. O.; Kleindienst, T. E.; Jaoui, M.; Edgerton, E. S.; Tanner, R. L.; Shaw, S. L.; Zheng, M.; Knipping, E. M.; Seinfeld, J. H. Influence of aerosol acidity on the chemical composition of secondary organic aerosol from β-caryophyllene. *Atmos. Chem. Phys.* **2011**, *11*, 1735−1751.
(43) Perri, M. J.; Lim, Y. B.; Seitzinger, S. P.; Turpin, B. J. Organosulfates from glycolaldehyde in aqueous aerosols and clouds: Laboratory studies. *Atmos. Environ.* **2010**, *44* (21−22), 2658−2664.
(44) Lim, Y. B.; Tan, Y.; Perri, M. J.; Seitzinger, S. P.; Turpin, B. J. Aqueous chemistry and its role in secondary organic aerosol (SOA) formation. *Atmos. Chem. Phys.* **2010**, *10* (21), 10521−10539.
(45) Curry, L. A.; Tsui, W. G.; McNeill, V. F. Technical note: Updated parameterization of the reactive uptake of glyoxal and methylglyoxal by atmospheric aerosols and cloud droplets. *Atmos. Chem. Phys.* **2018**, *18* (13), 9823−9830.
(46) Zhang, Z.; Lin, Y. H.; Zhang, H.; Surratt, J. D.; Ball, L. M.; Gold, A. Technical Note: Synthesis of isoprene atmospheric oxidation products: isomeric epoxydiols and the rearrangement products cis- and trans-3-methyl-3,4-dihydroxytetrahydrofuran. *Atmos. Chem. Phys.* **2012**, *12* (18), 8529−8535.
(47) Donahue, N. M.; Robinson, A. L.; Trump, E. R.; Riipinen, I.; Kroll, J. H. Volatility and Aging of Atmospheric Organic Aerosol. In *Atmospheric and Aerosol Chemistry. Topics in Current Chemistry*; McNeill, V., Ariya, P., Eds.; Springer: Berlin, Heidelberg, 2012; Vol. *339*, pp 97−143.
(48) Donahue, N. M.; Henry, K. M.; Mentel, T. F.; Kiendler-Scharr, A.; Spindler, C.; Bohn, B.; Brauers, T.; Dorn, H. P.; Fuchs, H.; Tillmann, R.; Wahner, A.; Saathoff, H.; Naumann, K. H.; Mohler, O.; Leisner, T.; Muller, L.; Reinnig, M. C.; Hoffmann, T.; Salo, K.; Hallquist, M.; Frosch, M.; Bilde, M.; Tritscher, T.; Barmet, P.; Praplan, A. P.; DeCarlo, P. F.; Dommen, J.; Prevot, A. S.; Baltensperger, U. Aging of biogenic secondary organic aerosol via gas-phase OH radical reactions. *Proc. Natl. Acad. Sci. U. S. A.* **2012**, *109* (34), 13503−8.
(49) Hansen, A. M. K.; Kristensen, K.; Nguyen, Q. T.; Zare, A.; Cozzi, F.; Noejgaard, J. K.; Skov, H.; Brandt, J.; Christensen, J. H.; Strom, J.; Tunved, P.; Krejci, R.; Glasius, M. Organosulfates and organic acids in Arctic aerosols: speciation, annual variation and concentration levels. *Atmos. Chem. Phys.* **2014**, *14* (15), 7807−7823.
(50) Ding, X.; He, Q.-F.; Shen, R.-Q.; Yu, Q.-Q.; Zhang, Y.-Q.; Xin, J.-Y.; Wen, T.-X.; Wang, X.-M. Spatial and seasonal variations of isoprene secondary organic aerosol in China: Significant impact of biomass burning during winter. *Sci. Rep.* **2016**, *6*, 20411.
(51) Tan, Z.; Rohrer, F.; Lu, K.; Ma, X.; Bohn, B.; Broch, S.; Dong, H.; Fuchs, H.; Gkatzelis, G. I.; Hofzumahaus, A.; Holland, F.; Li, X.; Liu, Y.; Liu, Y.; Novelli, A.; Shao, M.; Wang, H.; Wu, Y.; Zeng, L.; Hu, M.; Kiendler-Scharr, A.; Wahner, A.; Zhang, Y. Wintertime photochemistry in Beijing: observations of ROx radical concentrations in the North China Plain during the BEST-ONE campaign. *Atmos. Chem. Phys.* **2018**, *18* (16), 12391−12411.
(52) Kim, S.; VandenBoer, T. C.; Young, C. J.; Riedel, T. P.; Thornton, J. A.; Swarthout, B.; Sive, B.; Lerner, B.; Gilman, J. B.; Warneke, C.; Roberts, J. M.; Guenther, A.; Wagner, N. L.; Dubé, W. P.; Williams, E.; Brown, S. S. The primary and recycling sources of OH during the NACHTT-2011 campaign: HONO as an important OH primary source in the wintertime. *Journal of Geophysical Research: Atmospheres* **2014**, *119* (11), 6886−6896.

DOI: 10.1021/acs.est.9b02628
Environ. Sci. Technol. 2019, 53, 6192−6202

(53) Lelieveld, J.; Gromov, S.; Pozzer, A.; Taraborrelli, D. Global tropospheric hydroxyl distribution, budget and reactivity. *Atmos. Chem. Phys.* **2016**, *16* (19), 12477−12493.
(54) Xing, L.; Wu, J.; Elser, M.; Tong, S.; Liu, S.; Li, X.; Liu, L.; Cao, J.; Zhou, J.; El-Haddad, I.; Huang, R.; Ge, M.; Tie, X.; Prévôt, A. S. H.; Li, G. Wintertime secondary organic aerosol formation in Beijing−Tianjin−Hebei (BTH): contributions of HONO sources and heterogeneous reactions. *Atmos. Chem. Phys.* **2019**, *19* (4), 2343−2359.
(55) Hendrick, F.; Müller, J. F.; Clémer, K.; Wang, P.; De Mazière, M.; Fayt, C.; Gielen, C.; Hermans, C.; Ma, J. Z.; Pinardi, G.; Stavrakou, T.; Vlemmix, T.; Van Roozendael, M. Four years of ground-based MAX-DOAS observations of HONO and NO_2 in the Beijing area. *Atmos. Chem. Phys.* **2014**, *14* (2), 765−781.

DOI: 10.1021/acs.est.9b02628
Environ. Sci. Technol. 2019, 53, 6192−6202